Available online at www.sciencedirect.com
SCIENCE DIRECT
Journal of Power Sources 158 (2006) 287–294
JOURNAL OF POWER SOURCES
www.elsevier.com/locate/jpowsour

Modeling of thermal stresses and probability of survival of tubular SOFC

Arata Nakajo [a,*], Christoph Stiller [b], Gunnar Härkegård [c], Olav Bolland [b]

[a] *Laboratory for Industrial Energy Systems (LENI), Faculty of Engineering, Swiss Federal Institute of Technology, 1015 Lausanne, Switzerland*
[b] *Department of Energy and Process Engineering, Norwegian University of Science and Technology, Trondheim N-7491, Norway*
[c] *Department of Engineering Design and Materials, Norwegian University of Science and Technology, Trondheim N-7491, Norway*

Received 30 May 2005; received in revised form 16 August 2005; accepted 6 September 2005
Available online 19 October 2005

Abstract

The temperature profile generated by a thermo-electro-chemical model was used to calculate the thermal stress distribution in a tubular solid oxide fuel cell (SOFC). The solid heat balances were calculated separately for each layer of the MEA (membrane electrode assembly) in order to detect the radial thermal gradients more precisely. It appeared that the electrolyte undergoes high tensile stresses at the ends of the cell in limited areas and that the anode is submitted to moderate tensile stresses. A simplified version of the widely used Weibull analysis was used to calculate the global probability of survival for the assessment of the risks related to both operating points and load changes. The cell at room temperature was considered and revealed as critical. As a general trend, the computed probabilities of survival were too low for the typical requirements for a commercial product. A sensitivity analysis showed a strong influence of the thermal expansion mismatch between the layers of the MEA on the probability of survival. The lack of knowledge on mechanical material properties as well as uncertainties about the phenomena occurring in the cell revealed itself as a limiting parameter for the simulation of thermal stresses.

Keywords: Solid oxide fuel cell; Tubular; Thermal stresses; Model

1. Introduction

The fossil fuel resources mainly used for power production are limited and cause environmentally harmful emissions. Furthermore, its use is suspected to cause global warming. Therefore, its judicious use appears important. The solid oxide fuel cell (SOFC) is a direct conversion process, which allows the production of electricity with high efficiency while maintaining pollutant emission at low level. Moreover, the SOFC technology is now far beyond the theoretical state. Indeed, prototypes have proven its ability to achieve the conversion of fuel into electricity with high efficiency, especially in the case of a SOFC and gas turbine hybrid system. The next step is commercialization, which may imply a drop of the specific cost and extended lifetime.

The major limitation to lifetime comes from the degradation of the materials, which is due to the aggressive environment related to operation conditions. A decrease of the performance of the cell is observed as well as structural failure. The knowledge of the stress field in the cell is therefore of main interest. The sintering phase during the manufacturing process, combined with the mismatch between the coefficients of thermal expansion (CTE) of the materials of the membrane electrode assembly (MEA) induces residual stresses in the cell. During operation, thermal gradients cause additional stresses and chemically induced stresses occur if interconnectors sensitive to oxygen activity gradient are used. The consequence of these phenomena is mainly delamination and thermal cracking in the critical layers of the MEA. Additional research is needed in order to quantify and predict the contribution of the thermal stresses to the failure of the cell. The operating condition of the cell can be adjusted by a suitable control strategy. The challenge is to maximize in particular the efficiency with respect to lifetime.

Two types of studies of thermal stresses in SOFC can be found in the literature. The first one focuses on the residual stresses in the cell at room temperature. Finite-element analysis is compared to experimental measurements in order to estimate its

* Corresponding author at: LENI-ISE-STI-EPFL, Bât. ME A2, Station 9, CH-1015 Lausanne. Tel.: +41 21 693 3505; fax: +41 21 693 3502.
E-mail addresses: arata.nakajo@epfl.ch (A. Nakajo), christoph.stiller@ntnu.no (C. Stiller), gunnar.harkegard@immtek.ntnu.no (G. Härkegård), olav.bolland@ntnu.no (O. Bolland).

0378-7753/$ – see front matter © 2005 Elsevier B.V. All rights reserved.
doi:10.1016/j.jpowsour.2005.09.004

Nomenclature

e	thickness (m)
E	Young's modulus (Pa)
m	Weibull modulus
P_s	probability of survival
P_f	probability of failure
r	radius (m)
u	displacement (m)
V_R	reference volume (m^3)

Greek letters

α	coefficient of thermal expansion, CTE (K^{-1})
λ	first Lamé coefficient
μ	second Lamé coefficient
ν	Poisson coefficient
σ_i	principal stresses, $i = 1, 2, 3$ (Pa)
σ_0	characteristic strength (Pa)
τ	temperature difference (K)
Ω	boundary

Indices

i	principal directions
j	radial, axial direction
r	radial direction
z	axial direction

suitability for stress simulation. Such studies were performed by Yakabe et al. [1], Atkinson and Selçuk [2] and Montross et al. [3]. The second situation of interest is operating conditions, which is known to cause the failure of the cell. For example, Yakabe et al. [4,5] and Selimovic et al. [6] have coupled their thermo-electrochemical model with a finite-element tool in order to simulate the stresses in the cell during operation.

Little research has been conducted in thermal stresses in SOFC up to now, compared to the ones in thermo-electrochemical modeling. Furthermore, there are many degrees of freedom in design, such as tubular or planar, anode or cathode supported. Therefore, no method to handle the problem has yet been clearly established which is generic, reliable and affordable in terms of modeling capabilities. Moreover, knowledge on the mechanical properties of the materials of the MEA is sparse. Other uncertainties remain in critical areas, such as the temperature at which no internal stresses occur or behavior of the bonds at the interfaces of the layers.

The purpose of the present work is to study the effects of the characteristics of the temperature profile on the stress field in a tubular cell during operation. The approach is to couple a thermo-electro-chemical model for the computation of the temperature profile with an additional module for the stress field. No feedback from the stress calculation to the thermo-electrochemical model exists. Particular attention was paid to the values of the radial thermal gradients in the cell, which required separate calculation of the solid heat balances for the MEA. The Weibull analysis is a common way to estimate the failure probability of ceramic materials. Several authors [3,6] mentioned that the local maxima of computed stresses might exceed the yield strength of the materials if realistic probabilities of survival are targeted. In this work, a simplified Weibull analysis was applied, which allowed studying the evolution of the probability of survival for several cases including both steady state and dynamic operation. An analysis of the sensitivity of the stresses on the mismatch between the layers' coefficients of thermal expansion was performed in order to provide indication of the mechanical requirements on the choice of SOFC materials.

2. Modeling

2.1. Mechanical model and assumptions

The thermo-electro-chemical SOFC model, which provides the temperature profile in the cell, has been described by Stiller et al. [7]. The model was implemented in gPROMS, an equation oriented process modeling tool [8]. It was enhanced in order to detect the radial thermal gradients with higher accuracy. Thus, the MEA model is improved by calculating each layer separately. The steam reforming, water gas shift and electrochemical reactions are assumed to take place at the interface between the electrolyte and the anode. The model of the tubular cell geometry is simplified to an axisymmetric one, which implies neglecting circumferential temperature variations and the interconnect. Fig. 1 depicts the geometry and provides the actual dimensions.

The stress field model is based on the static uncoupled linear thermoelastic theory. The modeling has been performed with gPROMS in order have both the thermo-electro-chemical model and the stress model in the same computational tool. This approach is convenient, especially during dynamic operation. The drawback is the limitation of gPROMS in modeling complex geometries and its lack of advanced meshing possibilities.

The modeling assumptions to keep computing time reasonable are

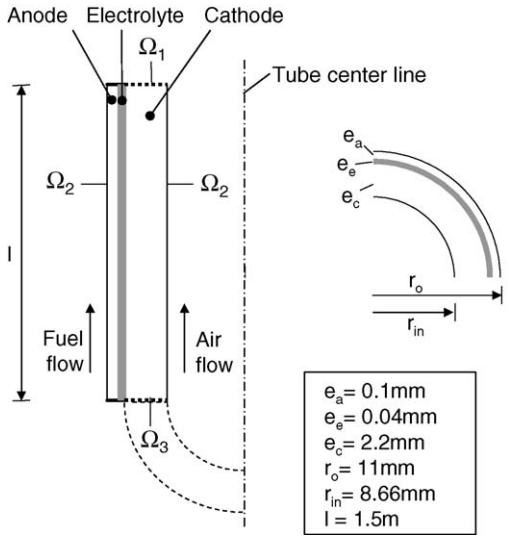

Fig. 1. Axisymmetric geometry of the cell used for modeling.

Table 1
Material properties of MEA components

	Young's modulus (GPa)	Poisson's coefficient	Coefficient of thermal expansion ($\times 10^{-6}$ K^{-1})	Characteristic strength (MPa)	Weibull modulus[a]
Cathode (LSM)	35 [20]	0.25 [20]	11.7 [17]	52 [12]	7 [12]
Electrolyte (YSZ)					
1073 K	183 [12]	0.313 [12]	10.8 [17]	256 [13]	5 [13]
298 K	212 [14]	0.32 [12]		332 [13]	5 [13]
Anode (Ni-YSZ)	57 [14]	0.28 [12]	12.2 [17]	115.2 [14]	6 [14]

[a] Only integer values could be implemented in gPROMS.

- The thermal expansion coefficients are constant over the considered range of temperature, e.g. values from the literature applicable over a range of 273–1300 K.
- The values of Young's modulus and Poisson's ratio at operating temperature are used when available, but their precise dependency on temperature is not modeled.
- The value of the zero stress temperature[1] is of the highest importance for the determination of the magnitude of the stresses. Major uncertainties remain in this area [1–3]. A uniform zero-stress temperature of 1400 K is used in the present work.
- The fixing of the cathode-supported cell is modeled by constraining the axial displacement at the boundary Ω_1 (Fig. 1). The boundary conditions at Ω_2 (Fig. 1) are determined by the pressure in the cell.
- The seal (Fig. 1) at the end is neglected due to meshing issues. The boundary Ω_3 (Fig. 1) is free.

The common Navier's equation is obtained by taking the displacement components u_j as the unknown of the fundamental equations of linear elastostatics. It is solved by the model under the previous assumptions. The resulting equation [9,10] is

$$\mu\nabla^2 u_j + (\lambda+\mu)u_{k,kj} - \frac{\alpha E}{1-2\upsilon}\tau_{,j} = 0 \quad (1)$$

The stress components are computed from the displacement fields. The three principal stresses,[2] σ_1, σ_2 and σ_3, are then determined with the principal invariants[3] method and used for a simplified version of the Weibull analysis [11]:

$$P_s = \prod_{i=1}^{3} \begin{cases} \exp\left(-\int_V \left(\frac{\sigma_i}{\sigma_0}\right)^m \frac{\mathrm{d}V}{V_\mathrm{R}}\right) & \sigma_i \geq 0 \\ 1 & \sigma_i < 0 \end{cases} \quad (2)$$

A simplification of the choice of the reference volume, V_R, was assumed. It considers the volume of the sample delimited by the outer ring of the so-called "ring on ring test", which was used in several sources on material properties [12–14]. Only few material configurations have been mechanically tested for the time being. They do not necessary correspond exactly to the materials used in tubular SOFC. The input data required for the whole process are listed in Table 1.

2.2. Verification against finite-element software (FEM)

gPROMS is not primarily designed to handle mechanical problems. Therefore its results were tested against those provided by a common FEM tool for stress computations, FEMLAB [15]. A typical temperature profile as it appears during operation was applied to a tube of 0.25 m length, made of layers of same diameter and thickness as the actual tubular cell. Fig. 2 depicts the comparison of the solution for the principal stresses of interest from gPROMS and FEMLAB. The agreement is considered as reasonable, especially when considering that the FEMLAB model uses more than 40 000 nodes, against only 738 for the gPROMS model.

2.3. Investigated cases

Both steady-state and dynamic operation of the SOFC were investigated. Several steady-state cases were chosen from a sequence of operating points designed in studies on part-load and load change with a model considering the SOFC and gas turbine hybrid system [7]. These operating points are characterized by the dimensionless shaft speed of the gas turbine (NDIM). High load is denoted by values around one. A particular feature of the pursued operation strategy is that it tries to keep the mean temperature of the SOFC at a fairly constant value over the range of NDIM 1.00 to NDIM 0.90. The fuel utilization[4] is close to 85% over the whole range. Furthermore, the stresses in the cell at room temperature were modeled by assuming a uniform temperature of 298 K in the cell.

The same model is used for dynamic simulation. Here, the input data, i.e. operating conditions, were assumed to vary linearly during a time interval of 60 s, since the model is limited to the SOFC and does not simulate the whole hybrid system. Only the SOFC conditions corresponding to the load cases were extracted from the hybrid system model. Two load changes were studied, NDIM 0.65 to NDIM 1.00 and NDIM 0.90 to NDIM 1.00. They represent changes of 75 and 15% of the rated power of the virtual hybrid system, respectively.

[1] *Zero stress temperature*: temperature at which no thermal stress act on the tube. In the SOFC, this coincides with the manufacturing temperature at which the layers are joined.
[2] *Principal stress*: stresses in the principal plane that is free of shear stresses.
[3] *Principal invariant*: coefficient in the eigenvalue problem required to establish the principal plane, the value of which is not altered by any rotation.
[4] *Fuel utilization*: fraction of the fuel which is oxidized in the fuel cell.

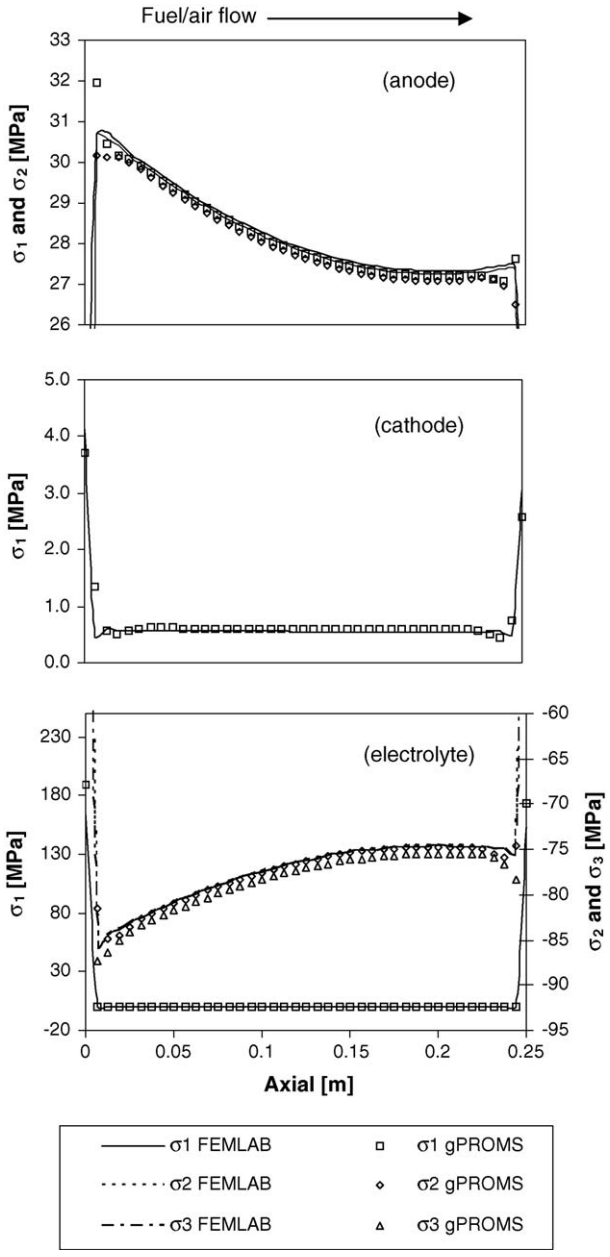

Fig. 2. Comparison of the thermal stresses in a tube computed by gPROMS and FEMLAB.

The sensitivity analysis considers a fixed value of the coefficient of thermal expansion of the anode, $12.2 \times 10^{-6}\,K^{-1}$, while those of the electrolyte and the cathode were allowed to vary in agreement with data found in the open literature. The large range of possible values is due to different doping methods. The Weibull modulus and strength, the Young's modulus and Poisson's coefficient were assumed to be constant. The analysis was performed at both high and low load, i.e. NDIM 1.00 and 0.65.

3. Results and discussion

3.1. Stress fields during operation

A comparison of the principal stresses at low and high load is depicted in Fig. 3. The stresses do not vary significantly in

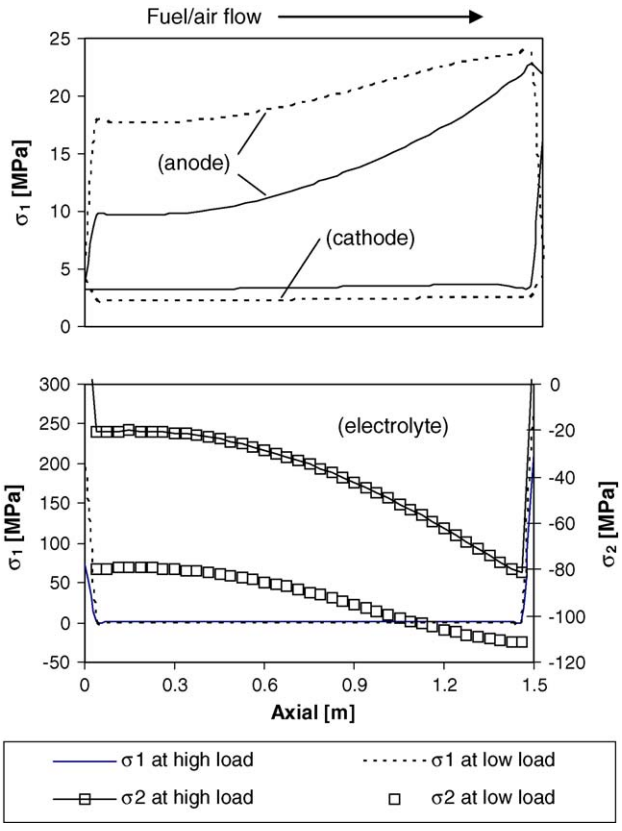

Fig. 3. Distribution of principal stresses at high and low load.

the radial direction. Two layers of the MEA undergo tensile stresses, the electrolyte and the anode. The variation of the shear stresses acting at the ends of the cell induces high tensile radial stresses in the electrolyte at the ends of the cell. They act in very small volume. The value exceeds 200 MPa, which is close to the characteristic strength of YSZ at the operating temperature. This behavior is opposite to that in the middle of the cell, where the smaller coefficient of thermal expansion of the electrolyte leads to compressive stresses. In the anode, both σ_1 and σ_2 are tensile, since the coefficient of thermal expansion of the Ni-YSZ cermet is the highest among the three layers. The stresses are highest at the fuel/air inlet, where the steam-reforming reaction induces a drop of the temperature.[5]

3.2. Steady-state cases

The observation of the specific values of the stress field cannot directly provide an indication of the risks associated with a particular operating point, since the failure of SOFC brittle materials are related to their defect structure. The probability of survival is a better criterion. Fig. 4 depicts its value for several operating points of the steady-state sequence. An optimum point for the global probability of survival occurs at intermediate load and is due to the opposite trends followed by the probabilities of survival in the layers. These are lower at low load in both

[5] In the fuel entering the cell, about 55% of the methane is reformed.

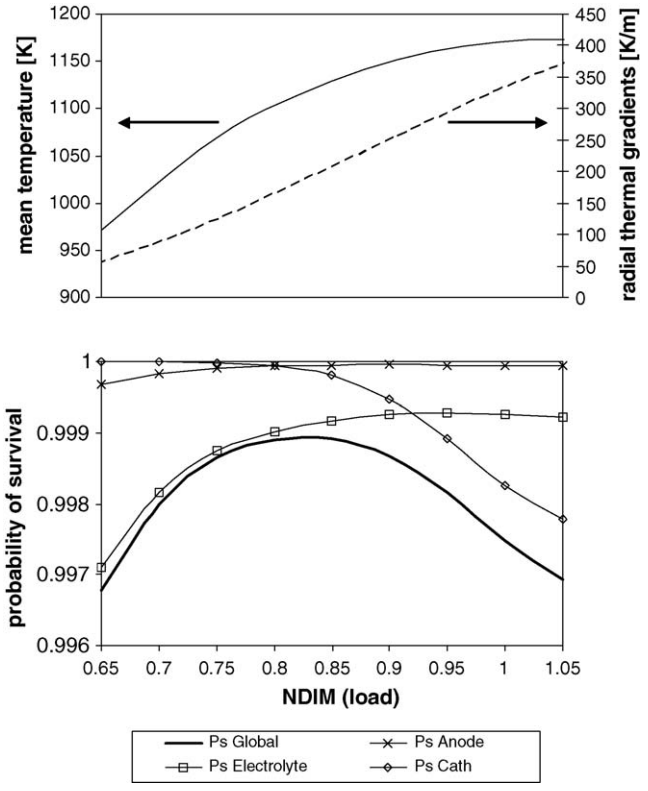

Fig. 4. Probabilities of survival as functions of the operating point during steady-state operation.

the electrolyte and the anode, due to the higher temperature difference τ induced by the low temperature in the cell. In the cathode, on the other hand, the probability of survival is lower at high load, when high radial thermal gradients act, which attain a local maximum at NDIM 1.0. Nevertheless, it must be noted that the results obtained here are restricted to a particular set of operating points and choice of material properties.

3.3. Dynamic simulations

The evolution of the probability of survival in the cell during both large and small load changes is depicted in Figs. 5 and 6, respectively. All load changes could be divided into a first phase with quickly changing probability of survival and a second phase where the probability of survival is slowly stabilizing.

From low load to high load, the increase of both mean temperature and temperature in the reforming area at the cell entrance induces an increase of the probability of survival during the first phase of the load change (Fig. 5). In the second phase, the probability of survival decreases due to the eventually increasing thermal gradients in the reforming area. At the transition point between both phases, the conditions are still close to the ones at low load, where the probability of survival in the cathode does not have a major contribution. Therefore, the trends are opposite during the reverse process: the quick decrease of the thermal gradients is during the first phase clearly effecting an increase of the probability of survival. The former is coupled to the increase of the temperature in the reforming area, which implies the same trend for the probability of survival of the electrolyte. In the second phase, the probabilities of survival of the anode and the electrolyte become dominant as they follow the decrease of the temperature.

At high load, the global probability of survival is dominated rather by the cathode than by the anode. Small load changes under these conditions are depicted in Fig. 6. The influence of the quick variations of the thermal gradients clearly appears on the evolution of the probability of survival, in both directions. The influence of the temperature acts through the same mechanisms

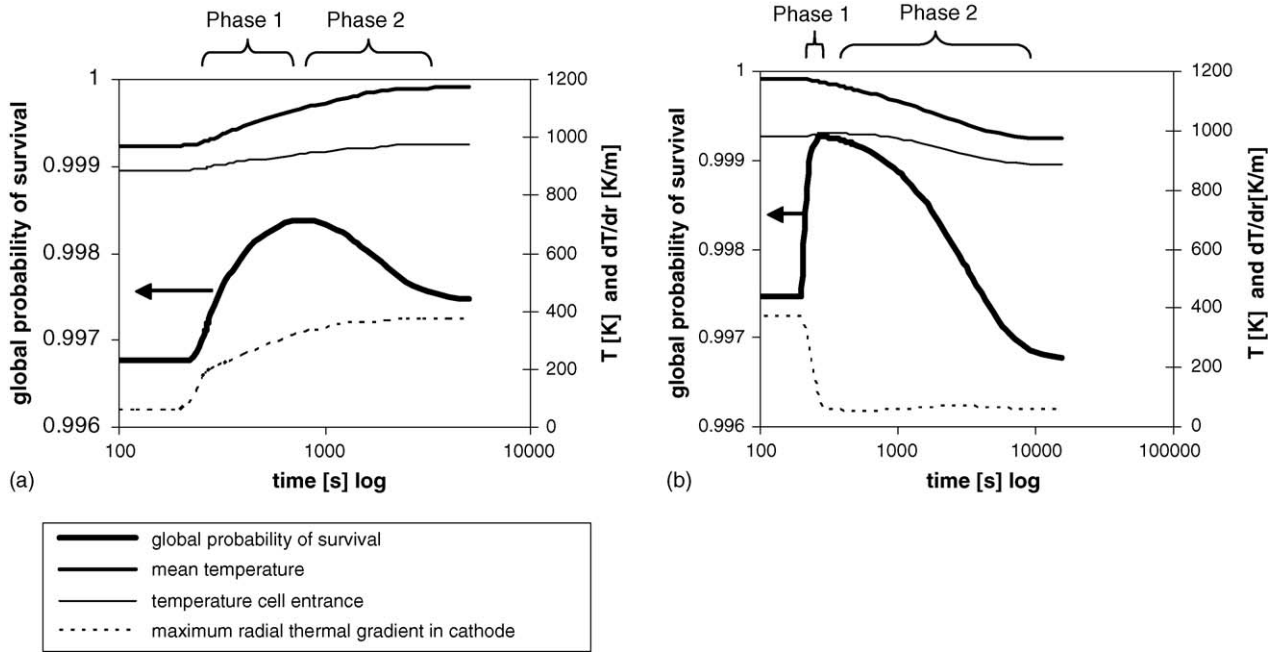

Fig. 5. Probabilities of survival, temperatures and gradients during load changes: (a) NIDIM 0.65 to NDIM 1.00; (b) NDIM 1.00 to 0.65.

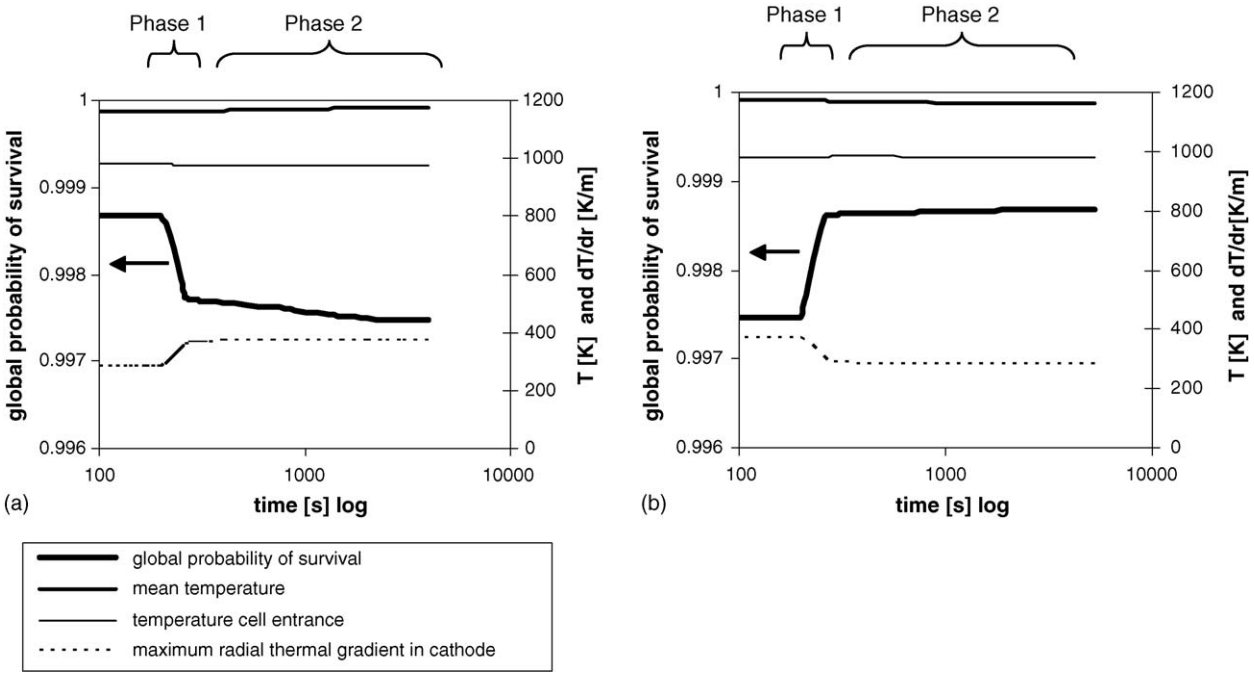

Fig. 6. Probabilities of survival, temperatures and gradients during load changes: (a) NIDIM 0.90 to NDIM 1.00; (b) NDIM 1.00 to 0.90.

as mentioned previously. From lower to higher load, the evolution of the probability of survival during the second phase is less dependent on the temperature. It is flatter during the decrease of temperature from NDIM 1.0 to NDIM 0.9. In contrast, the evolution of the radial thermal gradients is almost symmetric. The previous results do not show any intermediate drop of the global probability of survival during the investigated dynamic cases because of the combined effects of the temperature and the radial thermal gradients. This favorable combination may however not be generally true for all imaginable operation strategies of the system.

3.4. Sensitivity on mismatch between coefficients of thermal expansion

The differences between the layers' coefficient of thermal expansion mismatches are the primary cause of thermal stresses. High uncertainty exists about the CTE values. A multitude of values can be found in the literature, because of the wide possibilities in doping. In the present work, the range of coefficient of thermal expansion was found by literature review. In general, the CTE may be varied by modifying the material composition or other parameters, such as porosity [16]. Under these modifications, mechanical and electro-chemical properties of the materials would vary as well. This dependency was however not considered in the present sensitivity analysis; from Table 1 only the CTE is varied here. The CTE of the anode was kept constant at $12.2 \times 10^{-6}\,K^{-1}$ [17], while those of the electrolyte and the cathode were varied from $9.7 \times 10^{-6}\,K^{-1}$ [17] to $10.8 \times 10^{-6}\,K^{-1}$ [18] and from $11.3 \times 10^{-6}\,K^{-1}$ [16] to $12.8 \times 10^{-6}\,K^{-1}$ [17], respectively.

Fig. 7 depicts the results at both high and low load. The probability of survival is higher for high values of the coefficient of thermal expansion of the electrolyte, since the mismatch relative to both the cathode and the anode is reduced. The optimum set at low load differs slightly from the one at high load. Indeed, the cathode is the critical layer in the latter case and is prone to higher tensile stresses, if its coefficient of thermal expansion increases. In particular, the probability of survival is critical, when the coefficient of thermal expansion of the cathode exceeds that of the anode. This requirement is opposite to the one leading to the highest probabilities of survival in the anode. At low load, the contribution of the latter is larger and therefore induces a shift

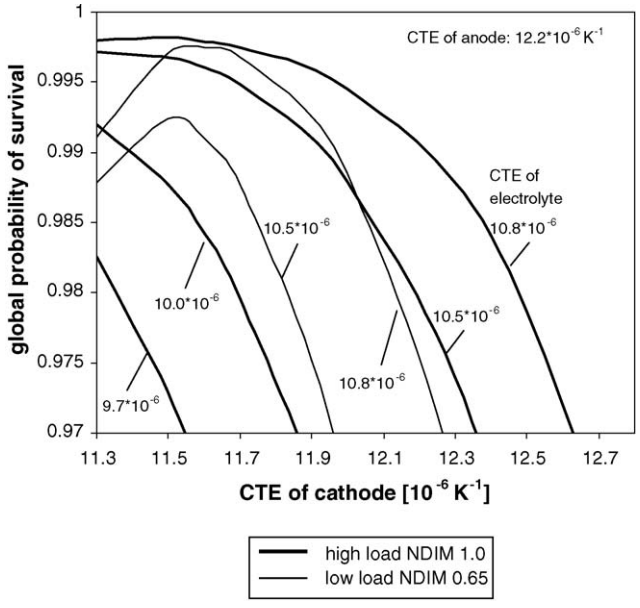

Fig. 7. Effect of cathode and electrolyte CTEs on the probability of survival at high and low load.

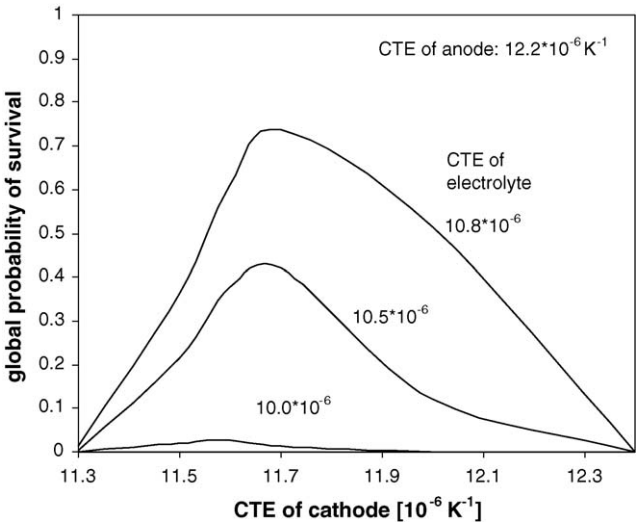

Fig. 8. Effect of cathode and electrolyte CTEs on the probability of survival at room temperature.

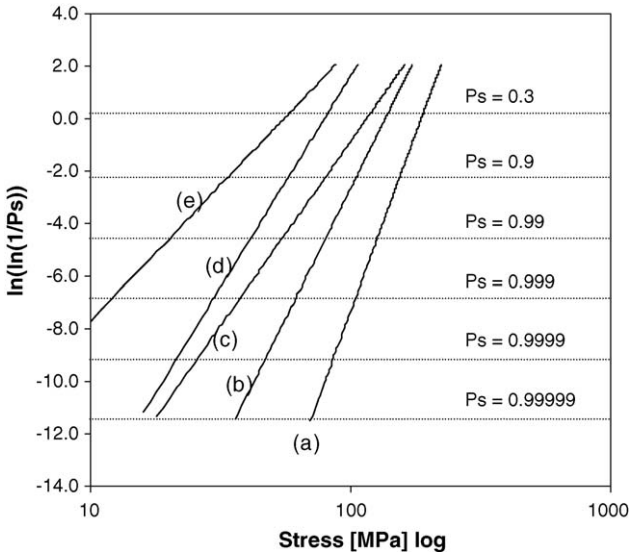

Fig. 9. Weibull plot of 75% Ni(O)-YSZ cermet (anode material) at room temperature: (a) unreduced [12]; (b) unreduced, porosity 0.06 [14]; (c) reduced, porosity 0.27 (used for the calculation in the present work) [14]; (d) reduced, porosity 0.36 [14]; (e) reduced, porosity 0.39 [14].

of the optimum point to higher cathode CTE compared with the case of high load. Furthermore, highest probabilities of survival can be achieved only for particular choices of CTE.

3.5. Room temperature case

The difference between the operating and the zero-stress temperature has been identified as a main driver of thermal stresses. From this point of view, room temperature appears as the most critical case. The shape of the stress fields shows the same global trend as during operation; that is high stresses at the ends of the cell in the electrolyte and tensile stresses in the whole anode.

Fig. 8 displays the result of a sensitivity analysis of the same kind as in Section 3.4. The optimum probability of survival over the considered CTE range is very low and located in a narrow regime.

3.6. Limitations

The comparison of the results presented in Sections 3.2–3.4 shows to some extent contradiction with the common observations, which indicate the failure of the cell during operation. However, the computation of stresses performed by Montross et al. [3] in the case of a planar cell at room temperature also indicates that probabilities of failure[6] as low as 10^{-5} cannot be achieved with the common SOFC materials. Nevertheless, this requirement is typical for applications targeted by the SOFC technology. Commercialization is obviously not possible under these conditions. Atkinson and Selçuk [12] pointed out the low values of the Weibull moduli as a limiting parameter. Ideally, these should be higher than 10.

Mechanical data for SOFC materials is still sparse. In particular, the dependency of the Young's modulus and the strength on temperature has not yet been precisely quantified. Its exploration is complicated by the wide possibilities in material composition, which mainly has to fulfill electro-chemical requirements. The manufacturing process also plays a major role; suitable sintering temperatures and processes are under investigation. The experimental data therefore depend on the supplier of the sample. The reduction of the anode material is another issue. Only few researchers [14] have consistently published its influence on the strength. This fact is visible in Fig. 9. It shows the probability of survival of 75% Ni(O)-YSZ over the stress at room temperature. The large discrepancies are partially due to different porosity and state, i.e. reduced and unreduced. However, in the most comparable case, the strength of the tested material differs significantly. For the preceding calculations, material (c) is used. The results presented in Sections 3.2–3.5 obviously change if material (a) or (b) was used. The dependency on porosity, which increases after reduction, amplifies the problem.

Other fundamental uncertainties remain. In particular, extended knowledge of the behavior of the bonds between the layers, as well as on the phenomena determining the value of the zero stress temperature are required. In the case of a tubular cell manufactured by electrochemical vapor deposition, the process requires the insertion of additional layers in order to prevent the growth of undesired phases [17]. A model assuming three layers joined to each other at a uniform temperature may not be refined enough to simulate the stresses in such tubular SOFC with satisfactory accuracy. The work of Li et al. [19] observed complex behavior of cell samples during their experiment for the analysis of crack density. In particular, reproducibility could not be achieved. The effect of the sintering temperature on the crack density was clearly observed. Unexpected behavior of the layers, such as compliance of the electrolyte is reported.

The experimentally observed mechanical failure of SOFC depends on the degradation of the materials due to the aggressive environment during operation. Studies on the evolution of

[6] Probability of failure: $P_f = 1 - P_s$.

the mechanical properties of the materials during the life of the SOFC are necessary to predict the SOFC life. Such phenomena have not been considered in the present study. The probability of survival, which has been used as test criterion, considers only the initial structure. Indeed, the current knowledge on the mechanical phenomena in SOFC does not allow modeling for the purpose of life assessment.

4. Conclusions

A model for calculating stresses was added to a thermo-electro-chemical model in order to simulate the thermal stresses in a tubular cell. For all studied cases, the stress fields display high tensile stresses in limited areas at the ends of the cell in the electrolyte and significant values in the whole anode. The latter is due to its high coefficient of thermal expansion. The magnitude of the stresses is higher at the fuel/air inlet, where the internal steam-reforming reaction induces a temperature drop. The comparison with FEMLAB, a suitable FEM tool, confirmed the ability of the modeling tool gPROMS to handle mechanical problems in particular cases, despite its limitation in meshing abilities, i.e. uniform, rectangular meshing and simple geometries.

The assessment of the risks related to particular operating points and load changes was performed through the probability of survival. The evolution of the latter is dependent on the temperature difference in both the anode and the electrolyte, whereas in the cathode, radial thermal gradients are most important. Therefore a maximum point for the value of the probability of survival of the cell is observed at intermediate load. Transient operation did not lead to any drop in the value of probability of survival. However, this favorable behavior may change when a different operation strategy is applied.

The greatest difference between the actual temperature and the sintering temperature occurs when the cell is at room temperature. The probability of survival calculated here reaches critical values, which might be acceptable for prototypes, but does not allow any commercialization. Significant improvement of the mechanical properties of the materials is required. This result is somewhat contradictory to the common observations, which rather indicate failure during operation. As a matter of fact, it shows the limitation of the thermal analysis alone and points out the importance of considering the degradation of the material during operation. Unfortunately, it appears that the published knowledge on material properties and complex phenomena occurring in the cell is not sufficient to allow any modeling for the purpose of lifetime assessment. Therefore, further studies should focus on the initiation and growth of cracks in SOFC and on improving the knowledge of material properties. An in-depth study of the influence of the choice of control strategy would also be of interest in order to find general criteria for stress-friendly operation.

Acknowledgement

We thank the Norwegian Research Council, Shell Technology Norway and Statkraft for their financial support.

References

[1] H. Yakabe, Y. Baba, T. Sakurai, Evaluation of residual stresses in a SOFC stack, J. Power Sources 131 (2004) 278–284.
[2] A. Atkinson, A. Selçuk, Residual stress and fracture of laminated ceramic membranes, Acta Mater. 47 (1999) 867–874.
[3] C.S. Montross, H. Yokokawa, M. Dokiya, Thermal stresses in planar solid oxide fuel cells due to thermal expansion differences, Br. Ceram. Trans. 101 (2002) 85–93.
[4] H. Yakabe, T. Ogiwara, M. Hishinuma, I. Yasuda, 3-D model calculation for planar SOFC, J. Power Sources 102 (2001) 144–154.
[5] H. Yakabe, I. Yasuda, Model analysis of expansion behavior of $LaCrO_3$ interconnector under solid oxide fuel cell operation, J. Electrochem. Soc. 150 (2003) A35–A45.
[6] A. Selimovic, M. Kemm, T. Torisson, M. Assadi, Steady state and transient thermal stress analysis in planar solid oxide fuel cells, J. Power Sources 145 (2005) 463–469.
[7] C. Stiller, B. Thorud, O. Bolland, Safe dynamic operation of a simple SOFC/GT hybrid system, ASME Turbo Expo, 2005-GT-68481.
[8] gPROMS (General Process Modelling and Simulation Tool), v.2.3.4, Process Systems Enterprise Ltd., London, http://www.psenterprise.com/.
[9] N. Noda, R.B. Hetnarski, Y. Tanigawa, Thermal Stresses, 2nd ed., Talyor & Francis, New York, 2002.
[10] S.P. Timoshenko, J.N. Goddier, Theory of Elasticity, 3rd ed., McGraw-Hill, Auckland, 1988.
[11] W. Weibull, A statistical theory of the strength of materials, Proc. Roy. Swed. Inst. Eng. Res. 151 (1939) 1–45.
[12] A. Atkinson, A. Selçuk, Mechanical behavior of ceramic oxygen ion-conducting membranes, Solid State Ionics 134 (2000) 59–66.
[13] F.L. Lowrie, R.D. Rawling, Room and high temperature failure mechanisms in solid oxide fuel cell electrolyte, J. Eur. Soc. 20 (2000) 751–760.
[14] M. Radovic, E. Lara-Curzio, Mechanical properties of tape cast nickel-based anode materials for solid oxide fuel cells before and after reduction in hydrogen, Acta Mater. 52 (2004) 5747–5756.
[15] FEMLAB Multiphysics modeling, v.3, COMSOL group, Sweden, http://www.femlab.com/in.
[16] M. Mori, Effect of B-site doping on thermal cycle shrinkage for $La_{0.8}Sr_{0.2}Mn_{1-x}O_{3+\delta}$ perovskites, Solid State Ionics 174 (2004) 1–8.
[17] N.Q. Minh, T. Takahashi, Science and Technology of Ceramic Fuel Cells, Elsevier, 1995.
[18] V.V. Kharton, F.M.B. Marques, A. Atkinson, Transport properties of solid oxide electrolyte ceramics: a brief review, Solid State Ionics 174 (2004) 135–149.
[19] W. Li, K. Hasinka, M. Seabaugh, S. Swartz, J. Lannutti, Curvature in solid oxide fuel cells, J. Power Sources 138 (2004) 145–155.
[20] N.M. Sammes, Yanhai Du, The mechanical properties of ceramic materials for solid oxide fuel cells, Electrochem. Proc. 97 (18) (2000) 671–679.